JOURNAL OF MATERIALS SCIENCE 19 (1984) 1446–1455

Low temperature deformation behaviour of ASTM A-203D nuclear structural steel

T. K. SINHA, J. K. CHAKRAVARTTY, S. L. WADEKAR, M. K. ASUNDI
Metallurgy Division, Bhabha Atomic Research Centre, Bombay, 400085, India

The steel A-203D in martensitic, tempered martensitic and ferritic–pearlitic microstructural conditions, was deformed in tension at temperatures between 77 to 300 K and at a strain rate of 6.67×10^{-5} sec^{-1}. The thermal component of the flow stress and the activation parameters were measured as a function of temperature. It was observed that the microstructure did not affect either the thermal part of the flow stress (σ^*) or the activation parameters (V^* and ΔH) and that its effect was felt only on the athermal component (σ_μ) of the flow stress. Further the relations of the activation parameters with stress, strain and temperature were found to be consistent with Dorn–Rajnak theory of Peierls mechanism of plastic deformation. In addition measurements of slow-bend and impact transition were also carried out for ferritic–pearlitic structure. Based on these observations, it is shown that the impact transition temperature of this structure can be emperically correlated with the thermal activation parameters.

1. Introduction

The low temperature deformation of bcc metals and their alloys has been the subject of numerous investigation [1–14]. Although for this group of metals, there is a lack of consensus on the rate controlling mechanism at low temperatures, a large number of studies support the view point that the inherent lattice or Peierls–Nabarro (P–N) hardening is the rate-controlling process. As regards the studies on iron and its alloys [7–21], it is observed that the majority of the investigations have so far studied pure metal or dilute alloys, probably because the primary concern has been the elucidation of a fundamental mechanism of flow and fracture. As a result technologically more important materials, such as commercial steels, have received far less experimental attention [17–21].

Wynblatt and Dorn [17] studied the low temperature plastic flow in low carbon manganese-steels. The temperature dependence of flow stress was found to be independent of interstitial impurity content. Below 160 K, the large temperature dependence of the flow stress was interpreted in terms of Dorn–Rajnak theory [1] of the Peierl mechanism of plastic deformation. Floreen [18] studied the deformation of martensite in low carbon, Ni–Cr steels. The results obtained on the activation parameters at low temperature were similar to those reported in case of iron and low carbon steel thereby indicating that the rate-controlling mechanism was (P–N) stress. Owen *et al.* [19] studied the low temperature deformation of martensite in nickel steels. The activation volume and activation energy data were in good agreement with Peierls mechanism of plastic deformation. Harding [20] studied the temperature and strain rate dependence of flow and fracture behaviour of four alloy steels in normalized and quenched and tempered conditions. It was noted that for the two of the steels studied, a single rate controlling mechanism (probably P–N stress) could adequately describe the flow behaviour in the temperature range of 77 to 225 K.

Jin *et al.* [21] in their study on a marging steel compared the microstructure and mechanical properties of microduplex structure (which consisted of fine grained martensite with interspersed islands of retained austenite) with those of maraged martensitic structure. The microduplex

0022–2461/84 $03.00 + .12

structure showed a much smaller temperature and strain rate dependence of flow stress compared to martensitic structure. Further there was significant difference between the activation volumes and activation energies of the two microstructures. These results raise some controversy regarding the influence of microstructure on the low temperature deformation mechanism in steel. If for iron and steel, the rate controlling mechanism of plastic flow at low temperature be the (P–N) stress, the activation parameter should be independent of microstructures. Therefore, it appears that further studies on low temperature deformation behaviour of commercial steels, with particular reference to the influence of microstructures, are necessary.

Since the ductile to brittle transition temperature is strongly influenced by thermal and athermal components of yield stress [22], there has been a number of attempts [23, 24] to correlate the ductile–brittle transition temperature (DBTT) with the thermal activation parameters. Recently Gerberich *et al.* [25] have derived a ductile–brittle transition model for iron and Fe-binary alloys, which involves a large number of flow and fracture parameters. In the present study an attempt has been made to correlate DBTT with thermal activation parameters. This approach, which is probably closest to that proposed by Norstrom [26], enables computation of the cleavage fracture stress from the DBTT determined by impact test and thermal activation parameters determined by tension tests. The cleavage fracture stress so computed can then be compared with the cleavage stress experimentally determined by slow notch bend testing, using the general yield approach [27, 28].

The material used in this study is a ferritic steel of ASTM A-203D designation. This is of interest to designers of large reactor components such as endshields of PHW reactors, because of its low DBTT and its expected low enhancement of DBTT after irradiat ion.

The thermally activated deformation of this steel in quenched, and tempered and normalized conditions has been studied to characterize the influence of microstructure on the mechanism of low temperature deformation. Since this steel is generally used in the normalized condition, the correlation of DBTT with thermal activation parameters has been attempted only for the normalized structure.

TABLE I Chemical composition of the steel

Element	(wt %)
C	0.13
Mn	0.52
Si	0.18
P	0.012
S	0.016
Ni	3.45
Cr	0.06
Mo	0.04
Sn	0.04
Al	0.01
Ti	0.01
V	0.01

2. Experimental procedure

2.1. Material

The steel used in the present study was obtained in the form of a hot-rolled plate of 50 mm thickness. This was further hot rolled (at 950° C) to a thickness of 4 mm and subsequently cold-rolled to 1 mm thick strips. The chemical composition of the steel was checked by spectrochemical method and is shown in Table I. The transversely oriented flat tensile specimens of 12.5 mm × 4.0 mm × 0.6 mm gauge dimension were machined from the strips. For hardness testing and microstructural studies, samples of 5.0 mm × 4.0 mm × 0.6 mm dimensions were punched out from the strips. For impact and slow notch bend testing, half-thickness, V-notch Charpy specimens (5 mm × 10 mm × 55 mm, 45° notch 2 mm deep) and bend specimens of 5 mm × 6 mm × 55 mm, 45° notch, 2 mm deep were machined from the hot rolled 50 mm thick plate in the transverse direction. The axis of the notch was normal to the plate surface.

2.2. Heat treatments

All austenitizing and tempering heat treatments were carried out in an electrically heated furnace with a temperature control better than ± 2° C. The samples for mechanical testing and structural studies were first ground and polished and then sealed in silica tubes (in a protective atmosphere of helium). The encapsulated samples were austenitized at 950° C for 30 min followed by water-quenching to produce martensite and air-cooling (normalizing) to produce a ferrite–pearlite structure. The as-quenched martensite was tempered at 550° C for 1 h. The hardness of martensite, tempered martensite and ferrite–pearlite structures were found to be VPN 450,

VPN 300 and VPN 190, respectively. These microstructures were designated as (M), (T–M) and (F–P).

2.3. Microstructural study

The microstructural examination of heat treated specimens were carried out by a optical microscopy as per standard metallographic technique.

2.4. Tensile test

The tensile specimens, suitably heat treated to produce the desired microstructures, were tested in tension using a floor model Instron testing machine, in the temperature range of 77 to 300 K. The low temperatures were obtained by using different baths such as liquid nitrogen, dry ice–methanol, ice–salt mixture and melting ice. The specimen was equilibrated for at least 20 min in the appropriate bath before testing and the temperature control was within $\pm 2^{\circ}$C. The normal strain rate adopted during these tests was 6.67×10^{-5} sec^{-1}. For strain rate change test, an instantaneous change from 6.67×10^{-5} to 6.67×10^{-4} sec^{-1} was used. The resulting changes in stress were measured for both upward and downward changes in strain rate and the two agreed well. The upward changes gave a small yield point in case of normalized structure (F–P) only. However this was not included in the measurement of the change of stress and the extrapolated steady state line was used. The strain rate change tests were carried out at various strain levels.

2.5. Impact test

The Charpy impact specimens heat treated to develop ferritic–pearlitic structure, were tested in the temperature range of 77 to 300 K to determined the impact energy curve as a function of test temperature. The mid-shelf energy value was taken to determine the ductile–brittle transition temperature (DBTT).

2.6. Slow bend test and the cleavage fracture stress (σ_F)

The general yield approach was used to determine the cleavage fracture stress. This involves slow notch bend testing, to determine the load at which plastically induced cleavage coincides with yielding spreading over the ligament under the notch. This load is used since the plastic constraint factor is known for this general yield condition. Following Knott [28] the general yield load (P_{GY}) can be obtained from the bending moment (M) in three or four point bending by

$$M_{GY} = 0.63\,\tau_y\,(W-a)^2 B \qquad (1)$$

where M_{GY} is given by $P_{GY}/2$ times the bending arm, $(W-a)$ is the ligament under the notch. B is the specimen thickness and shear yield stress is related to tensile yield

$$\tau_y = \sigma_y/3^{1/2} \qquad \text{(Von Mises)} \qquad (2)$$

Knowing the tensile yield stress of ferrite-pearlitic structure at various temperatures (Fig. 2), the general yield loads (P_{GY}) were determined as a function of test temperatures. Fracture loads (P_f) at each temperature were determined by slow notch bend testing, in three point bend employing same crosshead speed as used in tension test. The fracture load data was then superimposed on general yield loads against test temperature curve. The intersection point ($P_{GY} = P_f$) represented the slow bend transition temperature. The tensile yield stress at this temperature mutliplied by the plastic constraint factor gives the cleavage fracture stress (σ_F). Following Knott [28], a plastic constraint factor of 2.24 was used to compute the cleavage fracture stress of this structure.

3. Results and discussion

3.1. Microstructure

The microstructures produced by various heat treatments are shown in optical micrographs of Fig. 1. The normalizing has produced an equiaxed ferrite–pearlite structure (Fig. 1a). The mean ferrite grain diameter is about 15 μm but there is a wide distribution of grain sizes. The microstructure of quenched, and quenched and tempered material are typical lath martensite Fig. 1b, Fig. 1c. It is to be noted that the tempered structure Fig. 1c is more dark etching compared to as-quenched martensite, Fig. 1b. The parent austenite grain size has been estimated to be about 30 μm.

3.2. Temperature dependence of yield stress.

In several studies [1, 7–9, 11, 13, 15–17] on thermally activated deformation of bcc metals and alloys, the lower yield or initial flow stress is considered to consist of two components,

$$\sigma = \sigma^*(T, \dot{\epsilon}) + \sigma_\mu \qquad (3)$$

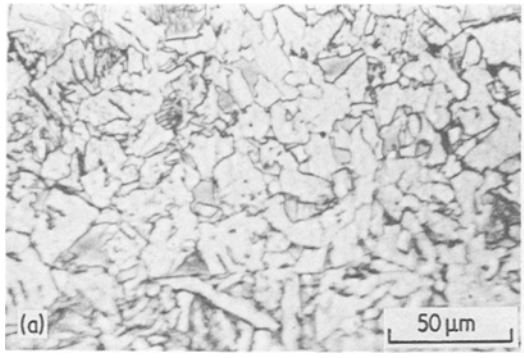

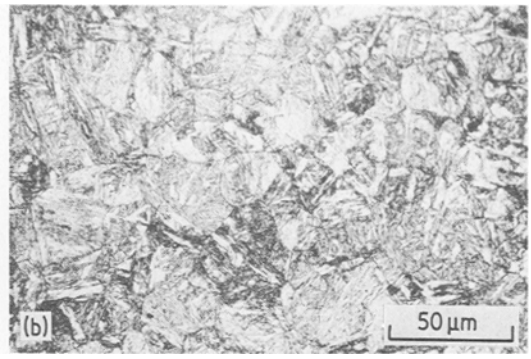

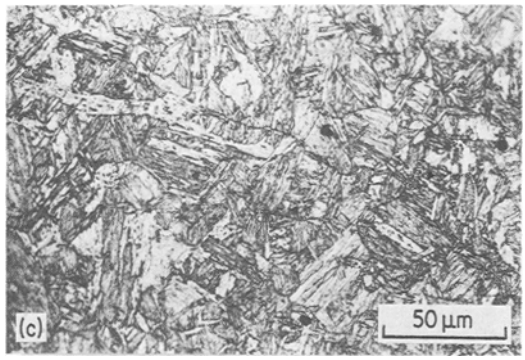

Figure 1 (a) Optical micrograph of normalized structure. (b) Optical micrograph of quenched structure. (c) Optical micrograph of quenched and tempered structure.

where σ_μ is the yield or the flow stress, σ^* is the effective stress which depends on the temperature and strain rate and is the athermal component which depends on the temperature only through the temperature dependence of the shear modulus.

The separation into thermal and athermal components of the stress can be achieved by evaluating the critical temperature T_c at which deformation becomes athermal and hence flow stress becomes equal to σ_μ. From the temperature dependence of the yield or the flow stress the values of stress differential $(d\sigma/dT)$ as a function of temperature can be obtained, and T_c can be determined by extrapolation of the stress differential to zero. The 0.2% yield stress of three microstructures as a function of temperature, are shown in the Fig. 2a. It is observed that in all structures the yield stress increases with decreasing test temperatures. Values of $(d\sigma/dT)_{\dot\epsilon}$, ϵ_p were computed from the Fig. 2a and plotted as a function of temperatures in Fig. 2b. The extrapolation to $(d\sigma/dT)_{\dot\epsilon}$, $\epsilon_p \to 0$ gives a T_c value close to 300 K (308 K). Smidt [16] observed that above 300 K, the temperature dependence of the yield stress of iron and its alloys is almost

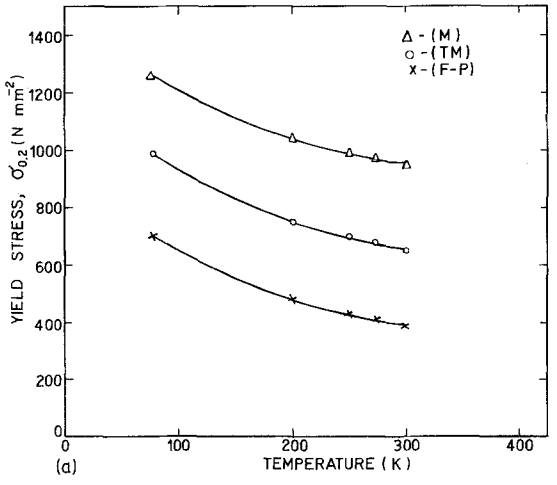

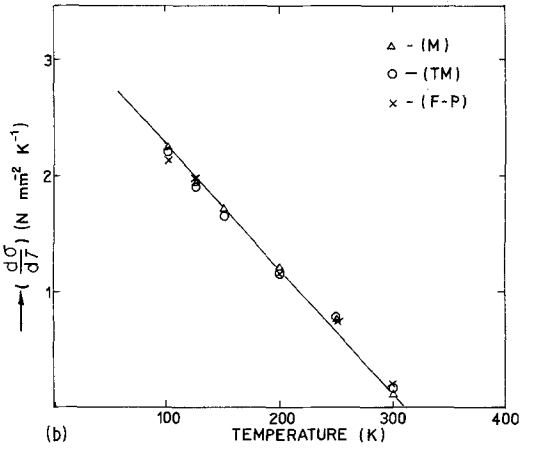

Figure 2 (a) The variation of yield stress of A-203D steel with temperature under various microstructural conditions. (b) Extrapolation of stress differential to zero to determine critical temperature, T_c, in A-203D steel.

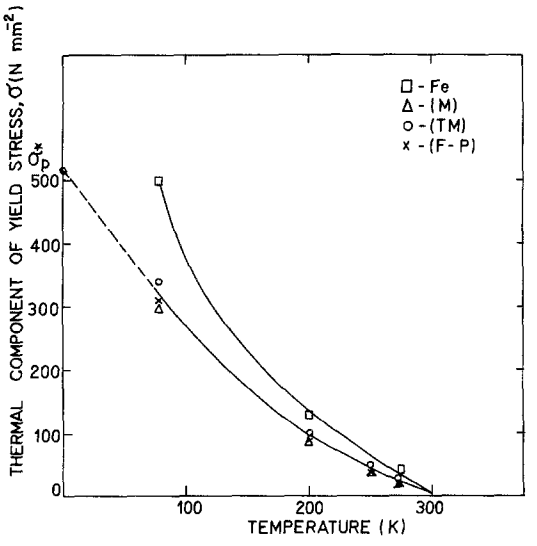

Figure 3 Effect of temperature on the thermal component of yield stress (σ^*) for A-203D steel As obtained from the Fig. 2.

zero. For Fe–4 wt % Ni. Chen *et al.* [15] have reported the T_c value less than 300 K. Thus within the limits of experimental accuracy, T_c for this steel can be taken as 300 K. Taking the yield stress at 300 K (σ_{300}) as an athermal component (σ_μ) of flow stress, the thermal part $\sigma^* = (\sigma_T - \sigma_{300})$ is plotted against temperature in the Fig. 3. The subscript T refers to absolute temperature. It is found (Fig. 3) that the thermal component of the yield stress of various microstructures are almost the same. It is therefore reasonable to take a mean value of σ^* as a representative value of the thermal part of the yield stress for all the microstructures. These results indicate that the influence of microstructure (and hence the influence of dissolved alloying elements) is only felt in the athermal part (σ_μ) of the yield stress of the three microstructures studied. The temperature dependence of the thermal component of the yield stress of unalloyed iron [9] is superimposed in the Fig. 3, for the purpose of comparison. It can be seen that although there is no significant difference between σ^*_{273}, σ^*_{250} and σ^*_{200} of unalloyed iron and those of various microstructures of this steel, the σ^*_{77} for unalloyed iron is clearly much higher than those for this steel under various heat-treated conditions (the difference being of the order of about 170 N mm^{-2}). The observed lowering of σ^* below 200 K may be due to solid solution softening.

3.3. Activation volume and activation energy

If a single thermally activated dislocation mechanism controls the rate of plastic deformation, then an activation volume (V^*) and an activation energy (ΔH) can be determined by the mathematical formulation derived by Seeger [29]–Conrad [9]

$$V^* = kT\left(\frac{\partial \ln \dot{r}}{\partial \tau}\right) \tag{4}$$

and

$$\Delta H = -kT^2\left(\frac{\partial \tau^*}{\partial T}\right)_{\dot{\gamma}}\left(\frac{\partial \ln \dot{\gamma}}{\partial \tau}\right)_T \tag{5}$$

where k is the Boltzmann constant, T is absolute temperature and $\dot{\gamma}$ is the shear strain rate. Both V^* and ΔH are functions of the resolved shear stress on the slip plane. Thus application of this rate theory to polycrystalline specimens may not be correct in the strict sense. The values of V^* and ΔH in polycrystalline specimens are average values. However, the review of the available data by Conrad [9] had led to the conclusions that, for bcc metals and alloys, the measured values of the activation energy and the activation volume at a particular stress for polycrystals and single crystals are essentially the same.

From the strain rate sensitivity and the temperature dependence of τ^*, the V^* and ΔH has been computed according to Equations 3 and 4. Fig. 4 shows the variation of activation volumes of various microstructures with nominal strain

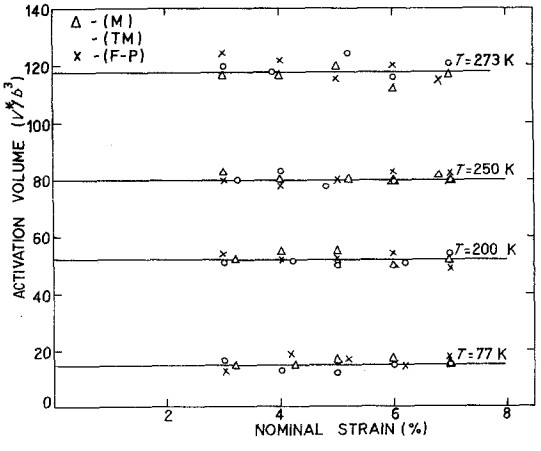

Figure 4 Activation volume as a function of nominal strain at different temperatures.

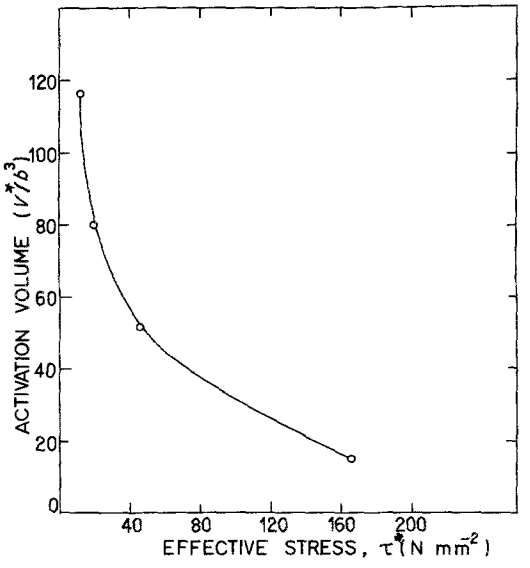

Figure 5 Activation volume as a function of effective shear stress.

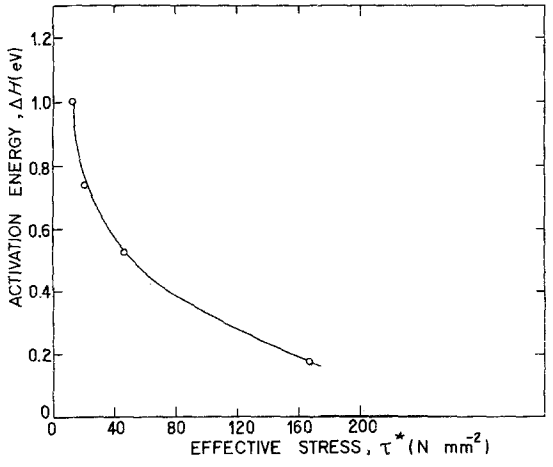

Figure 6 Activation energy as a function of effective shear stress.

at different temperatures. It is observed that at a particular test temperature, the value of the activation volumes of the three microstructures are almost identical thereby indicating that the activation volumes are independent of the microstructures. Since there was no appreciable variation in V^* of the various structures, a mean value has been taken to represent the activation volume of the three microstructure corresponding to a particular test temperature. It is also noted that the activation volumes of various microstructures are independent of strain, in the range of the test temperatures used in this investigation.

The variation of V^* as a function of τ^* (τ^* was taken to be $\sigma^*/2$) is shown in Fig. 5, the highest τ^* corresponds to 77 K. The results depicted in Fig. 4 and Fig. 5 are very similar to those obtained for iron and its alloys [9–11].

A number of mechanisms have been put forward to account for the increase in flow stress of bcc metals and alloys at low temperatures [15–19]. The one that best explains the observed effects in iron and a large number of its alloys, is the overcoming of P–N stress. First with this mechanism, the activation volume should be of the order of 1 to 100 $\mathbf{b}^3$ (**b** being Burgers vector) and should be independent of dislocation density (therefore of strain). The magnitude of V^*, its variation with temperature and effective stress and its invariance with strain, as observed in this study, are compatible with Peierls mechanism of plastic deformation. Since V^* and τ^* are independent of microstructures, the activation energy should also be independent of microstructure. Fig. 6 shows the variation of activation energy with effective shear stress τ^*, while Fig. 7 shows a plot of ΔH against T. It is seen (Fig. 7) that the relationship is linear up to 200 K and there is a departure of linearity above this temperature. Such deviation has been noted before [9, 19, 20] and may be due at least in part to the difficulty in measuring ΔH accurately at high temperature, where temperature and strain rate sensitivity are rather small. However, if these results are ignored, it may be concluded that at low temperatures (at least up to 200 K), a single rate controlling mechanism governs the plastic deformation of this steel. It should be

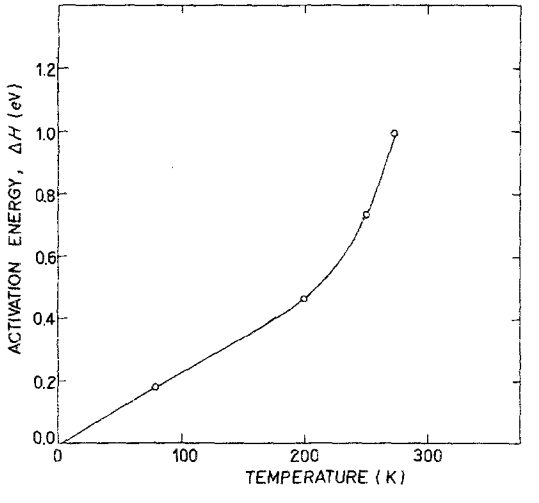

Figure 7 Activation energy as a function of temperature.

noted that the magnitude of activation energies of this steel at temperatures below 200 K are small compared to those observed for iron by other workers [10, 12, 13]. These results (decrease in σ^* and ΔH compared to those of iron) may be due to the solid solution softening phenomenon observed in Fe–Ni alloys by many investigators [12, 13, 15]. It should be noted that in the present study, the yield stresses of the three structures are always above those of pure iron, though thermal components of the yield stresses are smaller below 200 K. Therefore, it may be argued that there is no "true" solution softening in this alloy. However, similar observations were made in a thermal activation study [11] of Fe–Cu and Fe–Au alloys and the results were attributed to the solid solution softening caused by dissolved solute atoms. It may be reasonable, therefore, to interpret the present results in terms of solution softening caused by nickel in solid solution.

3.4. Comparison with Dorn–Rajnak model

Theoretical analysis of deformation by which dislocations sermount the Peierls stress hill involve the concept of the formation and the motion of double kinks in dislocations. According to the Dorn–Rajnak [1] model, the effective stress, τ^* is related to the temperature through a universal function,

$$\tau^* = \tau_p^* f(T/T_c) \qquad (6)$$

where τ_p^* is the Peierls stress, i.e. the effective stress at 0 K, T is the absolute temperature and T_c is the temperature for which $\tau^* = 0$. The theoretical relationship is given in Fig. 8 as a dimensionless plot of τ^*/τ_p against T/T_c.

It is noted from Fig. 8, that the data points of the present study can be fitted nicely with the theoretical curve. The line energy, Γ_0 of a disslocation is related in terms of the theory of Dorn–Rajnak [1] to the double kink nucleation energy, $2Uk$ and the Peierls stress τ_p^* by $(2\pi Uk)/(a\Gamma_0) = 5.7[(\tau_p^* ab)/(\pi\Gamma_0)]^{1/2}$ [7] where a is the distance between adjacent Peierls valleys. Using a value of $\Gamma_0 = 5 \times 10^{-9}$ N (5×10^{-4} dyne) from available literature [16], the experimentally determined value of $\tau_p^* = 260\,\mathrm{N\,mm^{-2}}$ and $a \simeq b$, the value of kink energy, $2Uk$ is estimated as 0.44 eV which agrees very well with the value estimated by Chen *et al.* [15] for Fe–4 wt % Ni alloy.

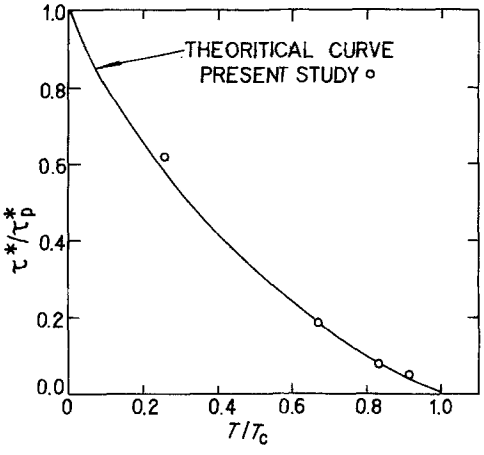

Figure 8 Temperature-dependent component of flow stress against temperature in dimensionless coordinates.

It therefore appears that the results of this investigation lends support to the Dorn–Rajnak [1] theory of Peierls mechanism of plastic deformation.

Duesberg *et al.* [30] have shown that the temperature dependence of yield stress and the thermal activation parameters of bcc metals can be satisfactorily explained with the help of a model of dissociated screw dislocation. This model has been compared critically with the Peierls model. It has been concluded that both models are physically similar and though there are differences in the functional dependence of ΔH on τ^*, it will be difficult to differentiate between the two on the basis of experimental measurements of the stress dependence of ΔH and V^*.

3.5. Impact energy

Impact energy of ferritic–pearlitic structure as a function of test temperature is shown in Fig. 9. The transition temperature (TDBTT), as defined, is found to be -100° C (173 K).

3.6. Slow notch bend transitions and cleavage fracture stress

Typical data of fracture (P_f) and general yield loads (P_{GY}) as function of temperature is shown in Fig. 10. It is noted that slow notch bend transition temperature T_D (SNB) for the ferritic–pearlitic structure is 112 K. The tensile yield stress corresponding to this temperature was determined from the data in Fig. 2. The appropriate plastic constraint factor (2.24) was then applied to compute the cleavage fracture stress σ_F.

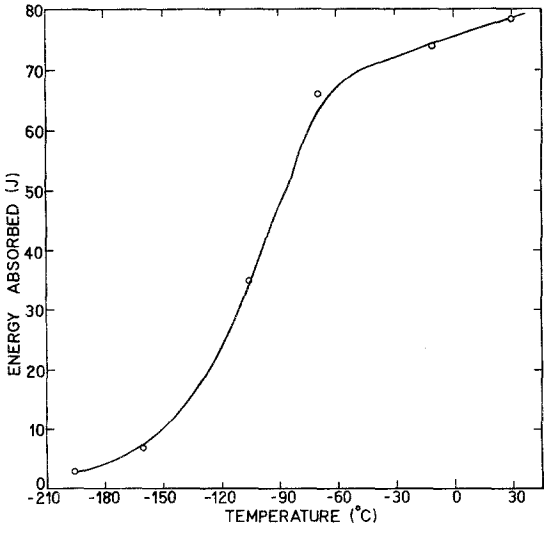

Figure 9 Charpy V-notch impact energy as a function of test temperature for normalized A-203D steel.

3.7. An attempt to correlate the activation parameters with ductile–brittle transition temperature

In a tension test, if σ_y and σ_{Ft} are the yield stress and fracture stress, the condition for a transition from ductile to brittle fracture can be written as

$$\sigma_y = \sigma_{Ft} \tag{8}$$

The yield stress is given by Equation 3 as

$$\sigma_y = \sigma^* + \sigma_\mu$$

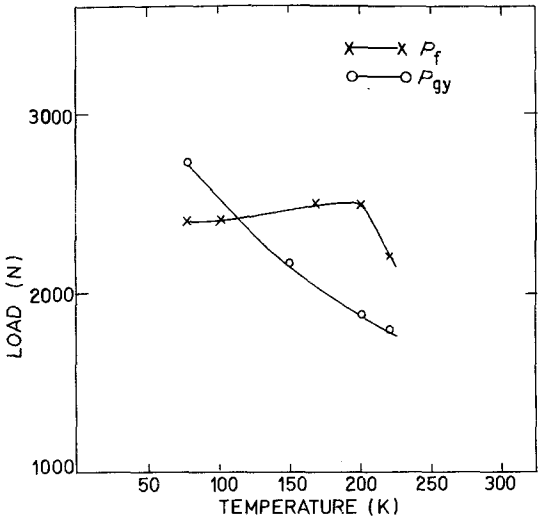

Figure 10 Determination of the slow notch bend transition from fracture (P_F) and general yield (P_{GY}) loads as a function of test temperature for normalized A-203D steel.

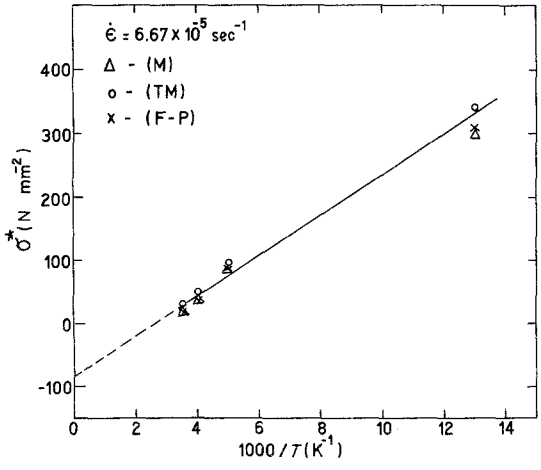

Figure 11 Thermal component of yield stress of A-203D steel as a function of reciprocal test temperature.

Following Seeger [31] and Conrad [32], σ^* can be expressed by the relationship

$$\sigma^* = A/T + B \log \dot{\epsilon} \tag{9}$$

where A and B are constants, T is the absolute temperature and $\dot{\epsilon}$ is the applied strain rate.

In Fig. 11, the σ^* values of Fig. 3 have been plotted as a function of $1/T$ and from the slope of the resulting straight lines, the value of A has been estimated to be 26 000 N mm^{-2} K. From the intercept of this line with σ^* axis, the corresponding value of B is found to be 20 N mm^{-2}, taking the applied strain rate as 6.67×10^{-5} sec^{-1}.

The ductile–brittle transition (T_0), i.e. the temperature at which $\sigma_{Ft} = \sigma_y$ can be obtained by combining the Equations 3, 8 and 9 such that

$$T_0 = \frac{A}{\sigma_{Ft} - \sigma_\mu - B \log \dot{\epsilon}} \tag{10}$$

Equation 10 refers to unnotched tensile testing. If this has to be used for impact tests, certain modifications are necessary. Although it is difficult to estimate the strain rate in an impact test, it is reasonable to take a value, $\dot{\epsilon} \simeq 10^3$ sec^{-1} [33]. Due to the stress concentration at the root of the notch the yield stress in Equation 8 will be raised by a plastic constraint factor q,

$$q\sigma_y = \sigma_{Ft} \tag{11}$$

Assuming that A, B and σ_μ remain the same as those determined in tensile tests, Equation 10 can be rewritten to describe ductile–brittle transition in impact as

$$\text{TDBTT} = \frac{A}{\sigma_{Ft}/q - \sigma_\mu - 3B} \qquad (12)$$

To test the validity of Equation 12 above, we attempted to estimate σ_{Ft} for this steel in the ferritic–pearlitic conditions. The TDBTT of this steel in the ferritic–pearlitic structure has been determined as -100° C, i.e. 173 K. Inserting this value in Equation 12 together with $A = 26\,000$ N mm^{-2} K, $B = 20$ N mm^{-2}, $\sigma_\mu = \sigma_y(300\text{ K}) = 390$ N mm^{-2} (Fig. 2a) and $q = 2.24$, we obtain $\sigma_{Ft} = 1345$ N mm^{-2}.

The slow notch bend transition has been found to be 112 K. The yield stress corresponding to this temperature is 620 N mm^{-2}. This multiplied by the plastic constraint factor (2.24) gives the cleavage fracture stress of 1388 N mm^{-2}. Thus the fracture stress computed by Equation 12, compares very well with the cleavage stress determined experimentally by slow notch bend tests. Further, these values compare favourably with the cleavage stress value of 1300 N mm^{-2} for Fe–4 wt % Ni alloy, reported by Gerberich *et al.* [25]. It therefore appears that Equation 12 gives a fairly good correlation between the TDBTT and the activation parameters.

4. Summary and conclusions

To our knowledge this work appears to be the first major attempt to study the influence of microstructures on the low temperature deformation behaviour of an alloy steel. The results of this study has adequately fulfilled this objective, although no attempt has been made to give any new theoretical interpretations of the data. It has also been shown that a simple correlation of the ductile–brittle transition with the thermal activation parameter does exist for a normalized structure of this steel. However further work on other microstructures of this steel and also on a variety of ferrous alloys should be done to verify the general applicability of this empirical relation. The following conclusions can be drawn from the results of this investigation.

(i) In A-203D nuclear structural steel, the thermal component of the flow stress σ^* and the activation parameters V^* and ΔH are independent of the microstructures. The microstructural contribution is felt only in the athermal part of the flow stress.

(ii) At low temperature the rate-controlling mechanism of plastic flow is the overcoming of P–N stress. Thus the deformation behaviour is practically identical to that of unalloyed iron.

(iii) The ductile–brittle transition temperature can be correlated with the thermal activation parameters.

Acknowledgements

This investigation forms a part of the general research programme on the mechanical properties of structural steels. We are grateful to the Head, Metallurgy Division for his keen interest in this work.

References

1. J. E. DORN and S. RAJNAK, *Trans. Met. Soc. AIME* **230** (1964) 1052.
2. J. W. CHRISTIAN and B. C. MASTERS, *Proc Roy. Soc (London)* **A281** (1964) 240.
3. R. J. ARSENAULT, *Acta Metall.* **15** (1967) 501.
4. D. F. STEIN, J. R. LOW and A. V. SEYBOLT, *ibid.* **14** (1966) 99.
5. R. L. FLEISCHER, *ibd.* **15** (1967) 1513.
6. J. E. DORN, "Dislocation Dynamics", edited by A. R. Rosenfield, G. T. Hahn, A. L. Berrent and R. I. Jaffee (McGraw Hill, New York, 1967) p. 27.
7. H. CONRAD, *J. Iron Steel. Inst.* **198** (1961) 364.
8. H. CONRAD and S. FREEDRICKS, *Acta Metall.* **10** (1962) 1013.
9. H. CONRAD, "The Relation Between the Structure and Mechanical Properties of Metals" (NPL Symposium, HMSO, London, 1963) p. 475.
10. Y. NAKADA and A. S. KEH, *Acta Metall.* **16** (1968) 903.
11. S. K. LAHIRI and M. E. FINE, *Met. Trans.* **1** (1970) 1495.
12. T. TANAKA and S. WATANABE, *Acta Metall.* **19** (1971) 999.
13. W. A. SPITZIG and W. C. LESLIE, *ibid.* **19** (1971) 1143.
14. W. A. SPITZIG, *Mater. Sci. Eng.* **12** (1973) 191.
15. Y. T. CHEN, D. G. ATTERIDGE and W. W. GERBERICH, *Acta Metall.* **29** (1981) 1171.
16. F. A. SMIDT Jr, Technical Report of Battelle-North West, BNWL-1045 (1969).
17. P. WYNBLATT and J. E. DORN, *Trans. AIME* **236** (1966) 1451.
18. S. FLOREEN, *ibid.* **236** (1966) 1429.
19. W. J. OWEN and M. J. ROBERTS, "Dislocation Dynamics", edited by A. R. Rosenfield, G. T. Hahn, A. L. Berrent and R. I. Jaffee (McGraw-Hill, New York, 1967) p. 357.
20. J. HARDING, *Met. Technol.* **1** (1977) 6.
21. S. JIN, D.HUANG and J. W. MORRIS, *Met. Trans.* **7** (1976) 637.
22. H. CONRAD, "High Strength Materials", edited by V. F. Zackay (John Wiley and Sons, New York, 1964) p. 436.
23. G. S. PISARENKO and A. J. KRASOWSKY, Second International Conference on Mechanical Behaviour of Materials, Special Volume (ASM, Metals Park,

Ohio, 1978) p. 348.
24. R. W. ARMSTRONG, "Fracture 1969", edited by P. L. Pratt, (Chapman and Hall, London, 1969) p. 314.
25. W. W. GERBERICH, Y. T. CHEN, D. G. ATTERIDGE and T. JOHNSON, *Acta Metall.* **29** (1981) 1187.
26. L. A. NORSTROM, *Scan. J. Metall.* **5** (1976) 41.
27. J. F. KNOTT, *J. Mech. Phys. Solids* **15** (1967) 97.
28. *Idem,* "Fundamentals of Fracture Mechanics" (Butterworths, London, 1973).
29. A. SEEGER, "Dislocation and Mechanical Properties of Crystals, Conference Volume", edited by J. C. Fisher, W. G. Johnston, R. Thomson and T. Vreelard (John Wiley and Sons, New York, 1957) p. 243.
30. M. S. DUESBERY and P. B. HIRCH, "Dislocation Dynamics", edited by A. R. Rosenfield, G. T. Hahn, A. L. Berrent and R. I. Jaffee (McGraw-Hill, New York, 1967) p. 57.
31. A. SEEGER, *Phil. Mag.* **45** (1954) 771.
32. H. CONRAD, *Acta Metall.* **6** (1958) 339.
33. G. E. DIETER, "Mechanical Metallurgy" (McGraw Hill, New York, 1961) p. 372.

Received 25 April
and accepted 15 August 1983